

Article

Potential Impacts of Sea Level Rise and Coarse Scale Marsh Migration on Storm Surge Hydrodynamics and Waves on Coastal Protected Areas in the Chesapeake Bay

Alayna Bigalbal, Ali M. Rezaie * , Juan L. Garzon and Celso M. Ferreira

Civil, Environmental, and Infrastructure Engineering, George Mason University, 4400 University Drive, MS 6C1, Fairfax, VA 22030, USA; abigalba@masonlive.gmu.edu (A.B.); jgarzon3@masonlive.gmu.edu (J.L.G.); cferrei3@gmu.edu (C.M.F.)

* Correspondence: arezaie@gmu.edu

Received: 16 May 2018; Accepted: 3 July 2018; Published: 16 July 2018



Abstract: The increasing rate of sea level rise (SLR) poses a major threat to coastal lands and natural resources, especially affecting natural preserves and protected areas along the coast. These impacts are likely to exacerbate when combined with storm surges. It is also expected that SLR will cause spatial reduction and migration of coastal wetland and marsh ecosystems, which are common in the natural preserves. This study evaluates the potential impacts of SLR and marsh migration on the hydrodynamics and waves conditions inside natural protected areas during storm surge. The study focused on four protected areas located in different areas of the Chesapeake Bay representing different hydrodynamic regimes. Historical and synthetic storms are simulated using a coupled storm surge (ADCIRC) and wave (SWAN) model for the Bay region for current condition and future scenarios. The future scenarios include different rates of local SLR projections (0.48 m, 0.97 m, 1.68 m, and 2.31 m) and potential land use changes due to SLR driven marsh migration, which is discretized in the selected preserve areas in a coarse scale. The results showed a linear increase of maximum water depth with respect to SLR inside the protected areas. However, the inundation extent, the maximum wave heights, and the current velocities inside the coastal protected areas showed a non-linear relationship with SLR, indicating that the combined impacts of storm surge, SLR, and marsh migration depend on multiple factors such as storm track, intensity, local topography, and locations of coastal protected areas. Furthermore, the impacts of SLR were significantly greater after a 1 m threshold of rise, suggesting the presence of a critical limit for conservation strategies.

Keywords: coastal protected areas; Chesapeake Bay; sea level rise; storm surge; marsh migration; ADCIRC+SWAN

1. Introduction

Both ocean water level records and satellite altimetry from the last century indicate a rise in global sea level [1–4]. In the next century sea level is expected to rise at a greater rate than during the past 50 years [5]. The Fifth Assessment Report (AR5) of the Intergovernmental Panel on Climate Change (IPCC) projected that from 1986–2005 to 2081–2100, the global mean sea level will rise by 0.26–0.55 m and by 0.45–0.82 m respectively, under the lowest (RCP2.6) and highest greenhouse-gas concentration scenarios (RCP8.5) [1]. The potential rise in sea level can largely affect coastal ecosystems through increased flooding, salinity, erosion, and loss of wetlands [6]. Although the loss of coastal wetlands can occur from various reasons [7], studies suggests that sea level rise (SLR) can reduce 22% of the world's coastal wetlands by the 2080s [8,9]. It is also estimated that 66% of coastal wetlands in 76 developing countries are at risk considering 1 m of SLR in the future [7]. Additionally, with projected hurricane

intensification over the next century [10,11], the combined effects of storm surge and SLR are likely to increase flood impacts in coastal areas [12].

Furthermore, SLR is most likely to exacerbate the impacts of storm surge by amplifying the total inundated area and maximum water levels [12–15]. Higher surge elevations, along with increasing wave heights driven by SLR [16], may result in increased tidal current and changes in shorelines [17]. The gradual shoreline recession will also reduce the wave energy dampening and increase the long-term erosion rates [18]. This will largely affect coastal wetlands and salt marshes containing plants and vegetation that can only withstand within a limited tidal range, salinity [19,20], and elevation range to mean sea level [21]. The sustainability of these natural habitats depends on the accretion rate at which they are vertically rising with respect to the rate of SLR [22]. If the water elevation is rising at a faster rate than the marsh is able to build in order to sustain vegetation, the marsh will begin to migrate inland [23]. Although some tidal wetlands are capable of vertical movement with small changes in sea level [20,24], higher increase in SLR will cause submergence and landward movement of marshes across the coastal landscape [24,25]. The incapacity of a migration could lead to the loss of the entire marsh and cause major land cover changes. Nonetheless, the physical response of these coastal lands to SLR is complex [26], and thus sustainability of wetlands in these protected lands will depend on multiple factors such as local geomorphology, sediment supply, vertical accretion, subsidence, and interaction between biotic and hydrologic processes [22].

While several studies [13,27–31] evaluated the impacts of storm surge and SLR on coastal lands and communities, their specific effect on protected lands in coastal areas, such as the Federal and State preservation areas, are less discussed. A recent study [32] looked at the potential exposure of coastal protected areas to SLR at a macro level and estimated that about 95% of the protected areas in the eastern United States (US) will be affected by a 0.92 m (3 ft.) of SLR. The study also suggested that adaptation policies for the protected areas should focus on a local scale. However, the study only assessed the impacts of inundation due to SLR. Another study [33] investigated the combined inundation risks from both storm surge and SLR on two northeastern coastal National Parks and found that their vulnerability to inundation varied according to the site location. The results of the study showed that the natural habitat with high-elevation settings is less vulnerable to inundation than the low-lying National Park site. Although the spatial scale of the studies is different, both studies have indicated a higher flood exposure and inundation risk to the coastal protected areas. However, rather than applying coastal numerical models to address the coastal hydrodynamic processes in the protected areas, both studies used a “bathtub” approach to estimate the inundation within the protected areas.

The protected areas along the coasts of the US are natural, undisturbed lands, which contain wetlands, forests, marshes, etc. and provide a range of ecosystem services. This includes water purification, storm surge attenuation, fish nurseries, carbon sequestration, and protection of wildlife habitat [34,35]. With changes in sea level, these ecosystems can become more vulnerable and lead to changes in the hydrodynamic and hydrological regimes [36,37] in the coastal wetlands. In this study, a coupled hydrodynamic and waves model, ADCIRC+SWAN [38–40], is applied for the Chesapeake Bay region to evaluate potential impacts of storm surge, SLR, and marsh migration to the hydrodynamic and wave responses in four coastal protected areas. One historical hurricane and two synthetic storms are simulated for a baseline condition and future SLR scenarios (0.48 m, 0.97 m, 1.68 m and 2.31 m of SLR) to compare and contrast the inundation extent, maximum water elevation, current velocities, and wave heights in the preserve areas. Based on the National Climate Assessment [41] and regional land subsidence rate [42], four local SLR projections are included in the modeling approach. Additionally, projected land use changes due to potential reduction and migration of coastal wetlands and marshes are included in the analysis. The objective is to use regional SLR and publicly available large geographical scale marsh migration projection data in regional coastal numerical models to explore how these land cover changes will impact the hydrodynamics and waves regimes during storm surge events in coastal protected areas in the future.

2. Methodology

2.1. Study Area

The Chesapeake Bay is located within the Mid-Atlantic regions of the east coast of the US (Figure 1). The Bay is surrounded by the coastal counties of Maryland (MD) and Virginia (VA), which has been identified as one of the “hot spot” coasts for SLR [43]. In addition, the bay areas are experiencing a higher rate of land subsidence than the accretion rate (Boon, 2010). The lower accretion rate in the Bay areas can exacerbate the impacts for wetlands and marshes that are located in the low-lying coastal landscape. A study by Beckett et al. [44] used surface elevation and accretion measurements in freshwater and brackish marshes in the Nanticoke estuary of the Chesapeake Bay and demonstrated that, on average, the wetland elevation has decreased by $1.8 \pm 2.7 \text{ mmyr}^{-1}$, which is at least 5 mmyr^{-1} below the rate at which global sea level is rising. Recent studies also suggest that due to SLR, Virginia can lose about 50% to 80% of its wetlands [45]. Additionally, a 0.92 m (3 ft.) rise in sea level can affect about 25.2% of the protected areas in Virginia and 24.3% in Maryland [32].

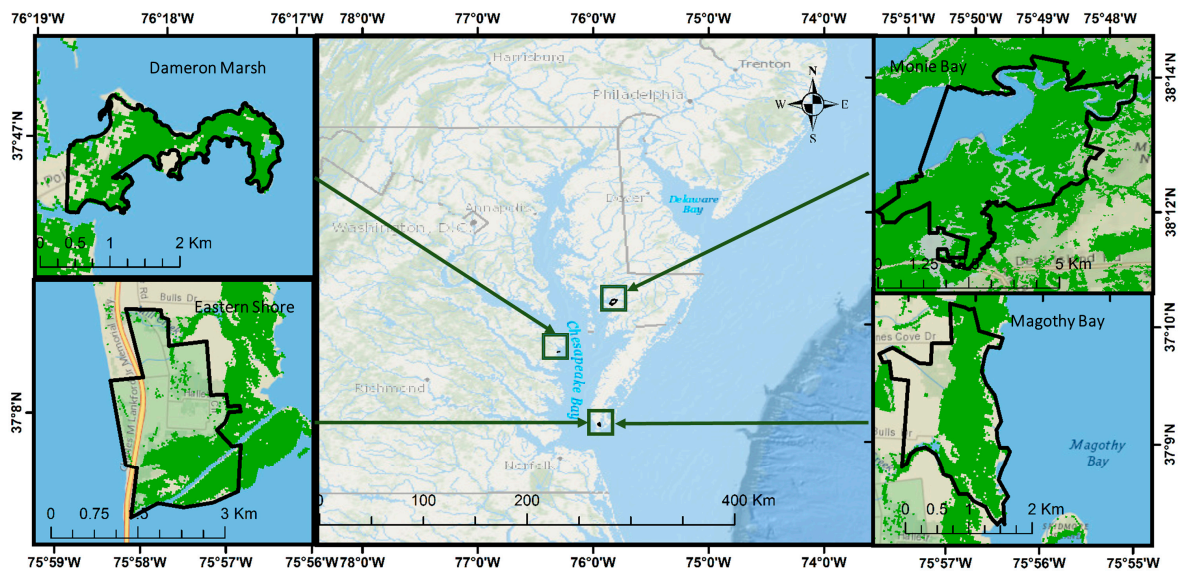


Figure 1. Location of the four study areas within the Chesapeake Bay (tidal wetlands and marshes areas are highlighted in green).

For this study, four protected areas in the Chesapeake Bay were selected due to their different exposure to the tides and surge along the Bay. Figure 1 shows the locations of the sites in the Bay and representative photographs collected during the study. The preserve areas are the Dameron Marsh Natural Area Preserve (DM), the Eastern Shore National Wildlife Refuge (ES), the Magothy Bay Natural Area Preserve (MGB), and the Monie Bay National Estuarine Research reserve (MB). Each site contains different types of wetlands and marshes presenting specific characteristics and increasing the research interest on these sites. For instance, Dameron Marsh is affected by an unbalanced sediment transport problem, highly eroding the north part and building up the southern portions. Eastern Shore and Magothy Bay are located at the southern portion of the Delmarva Peninsula and are highly exposed to storm surge. Monie Bay is the only site located at the mid-eastern side of the Bay, and additionally, it is used for numerous research projects on marsh ecology. It should be noted that terms such as “protected areas,” “preserve areas,” or “reserve areas” are interchangeably used in the literature referring to natural preserve areas. In this study, the term “preserve area” refers to each selected site, whereas “protected areas” is used to denote protected areas in general.

The selected preserve areas present the typical characteristics of tidal marshes in temperate regions, mainly composed of *Spartina alterniflora* in the lower marsh and *Spartina patens* in the upper

marsh [46]. This provides the opportunity to examine the impacts on storm-induced waves, currents, and water levels by a marsh with vegetation typical for the Mid-Atlantic region. The mean elevation of these lands varied with their locations along the Chesapeake Bay. Preserve areas located at the mouth of the Bay (Eastern Shore and Magothy Bay) have relatively lower elevation than the other two sites, which are located near the middle of the Bay. The total area, location, mean elevation, and types of vegetation in each preserve area are summarized in Table 1.

Table 1. Summary chart of the four study sites.

Study Area				
Reserve	Location	Land Area	Mean Elevation *	Vegetation ⁵
Dameron ¹ Marsh	Northumberland County, VA	1.3 km ² (316 Acre)	5.7 m	<i>Spartina alterniflora</i> , <i>Juncus roemerianus</i> , <i>Distichlis spicata</i> , <i>Scirpus robustus</i> , <i>Phragmites</i> , <i>Spartina patens</i>
Eastern ³ Shore	Delmarva Peninsula, Northampton County, VA	4.55 km ² (1123 Acre)	1.7 m	<i>Spartina alterniflora</i> , <i>Juncus roemerianus</i> , <i>Distichlis spicata</i> , <i>Spartina cynosuroides</i> , <i>Spartina patens</i>
Magothy ⁴ Bay	Northampton, VA	1.16 km ² (286 Acre)	1.7 m	<i>Spartina alterniflora</i> , <i>Juncus roemerianus</i> , <i>Distichlis spicata</i> , <i>Spartina cynosuroides</i> , <i>Spartina patens</i>
Monie ² Bay	Somerset County, MD	13.87 km ² (3426 Acre)	2 m	<i>Spartina alterniflora</i> , <i>Ruppia maritima</i> , <i>Spartina patens</i> , <i>Distichlis spicata</i> , <i>Juncus roemerianus</i>

* Mean Elevations are referred to NADV88. ¹ (DCR, 2005); ² (CBNERR-MD, et al.); ³ (“Easternshore”, 2005); ⁴ (“Magothy Bay Natural Area Preserve”, n.d.); ⁵ (Plant ES Natives Campaign).

2.2. Sea Level Rise in the Study Areas

In order to incorporate SLR in future scenarios, local SLR projections [42] for the Chesapeake Bay are used in this study. The local projections are derived from the synthesis and recommendations from National Climate Assessment (NCA) [41]. Based on global and regional assessment of past SLR trend and future IPCC emission scenarios, NCA prepared four possible SLR projections for managing the coastal resources in the US. Depending on different rates of SLR and ice sheet loss, these projections are considered as the lowest (or historic), low, high, and highest. Considering a constant regional subsidence rate of 2.7 mm/year, Mitchell et al. [42] derived four local SLR projections consistent to the national assessment. Due to low regional subsidence rate and higher rate of local SLR, the study [42] anticipated that subsidence rate for the region will be relatively constant [42]. Although this implies uncertainty in potential land use changes due to SLR, in order to capture a range of SLR and marsh migration impacts, we applied all four local projections in our study. The projected end of the century SLR values used in the study are provided in Table 2.

Table 2. Local sea level rise (SLR) projections at the end of the century for the Chesapeake Bay Regions and the nearest marsh migration scenario.

SLR Projections	Local SLR ¹	Marsh Migration Scenario ²
Historic	0.49 m (1.6 ft.)	0.61 m (2 ft.)
Low	0.98 m (3.2 ft.)	0.92 m (3 ft.)
High	1.68 m (5.5 ft.)	1.53 m (5 ft.)
Highest	2.32 m (7.6 ft.)	1.83 m (6 ft.)

¹ (Mitchell et al., [42]); ² (NOAA [47]).

2.3. Marsh Migration—Potential Land Cover Changes

The potential land use changes due to SLR driven marsh migration are collected from the NOAA SLR Viewer tool [47]. The tool estimates potential spatial reduction and migration of coastal wetlands and marshes through a “modified bathtub” approach that includes local and regional tidal range, tidal level and salinity [47]. The basic assumption is, with an increase in sea level, some marshes will move into the adjacent low-lying areas. Meanwhile, marshes unable to maintain their elevation relative to sea level will slowly submerge into open water or convert to an intertidal mudflat [20]. It also considers that, based on the varying frequency, salinity, and time of inundation, certain types of vegetation can exist and particular types of wetland will sustain within an established tidal range [48]. The projections allow wetlands and marshes to migrate into other vegetated canopies such as forested or agricultural lands. It should be noted that coastal physical processes such as erosion, subsidence, or ecological and geomorphologic changes are not included in the NOAA marsh migration projections, which oversimplify the complex processes and can impose uncertainty in their prediction. Although previous studies [49,50] have projected local scale distribution of marshes due to SLR using eco-geomorphologic models, there are trade-offs between acquiring fine scale marsh migration projection and simulating marsh evolution [51,52]. Therefore, this study utilized the NOAA projected marsh migration data for including the best publicly available regional scale coastal land use projection due to SLR induced marsh migration and reduction in a large-scale geographic region.

Also, note that the tool provides marsh migration projections from 0.31 m (1 ft.) to 1.83 m (6 ft.) of SLR with an increment of 0.3 m (1 ft.) of SLR. Therefore, to prepare future scenarios that integrates SLR projections with potential marsh migration, each SLR projection is combined with the closest SLR driven marsh migration projection. For example, in the end century “low” scenario, the projected rise in sea level is 0.96 m (3.2 ft.), while in the NOAA tool the land use change projection due to closest SLR value is available for 0.92 m (3 ft.). Thus, for modeling the “low” scenario, a 0.96 m of SLR is added in the model while the respective land use scenario is incorporated from a 0.92 m (3 ft.) SLR induced marsh migration projection. In Table 2, the correlation between each local SLR projections and nearest marsh movement or reduction scenario is outlined for the readers.

Additionally, Figure 2 demonstrates the projected land cover changes in the selected preserve areas due to marsh migration. The third column in Figure 2 shows the current land cover in the protected areas while the fourth and fifth columns show the projected land cover changes due to the “low” and “highest” SLR scenarios. It can be seen from the last two columns that with SLR, the existing salt-water marshes in the protected areas will either submerge into open water or convert to unconsolidated shore. For example, the second row on Figure 2 displays that with a 1.83 m (6 ft.) of SLR, the existing saltwater marshes in Dameron Marsh will submerge in the open water, while the freshwater wetlands can convert to brackish or transitional marshes. The current land use and land cover information is collected from NOAA’s Coastal Change Analysis Program (C-CAP) [53]. The details of different land cover types can also be found from the C-CAP database.

2.4. Modeling Storm Surge and Waves

The coupled version of the hydrodynamic model, ADCIRC [38,39] and wind wave model, SWAN [54], was applied to simulate the impacts of storm surge and SLR in the coastal lands. ADCIRC is a numerical model that computes depth-averaged water levels through the Generalized Wave Continuity Equation (GWCE) and currents through vertically integrated momentum equations [55]. SWAN [54] is a third-generation wave model for estimating wave parameters based on the wave action balance equation. The coupled version of ADCIRC+SWAN simulates the interaction of wind waves and circulation on the same numerical mesh and thus shares the same model boundary. ADCIRC computes the water levels, currents, and wind speeds at each time step and passes it to SWAN. The information is used in SWAN to calculate the wave parameters and wave radiation stress gradients which are further applied to force ADCIRC in the next time step [55,56]. Further details about the coupling processes can be found in [55,56]. In this study, the FEMA Region III Mesh (R3) [57] is used to simulate storm surge

in the Chesapeake Bay regions. The R3 Mesh was developed and validated by the United States Army Corps of Engineers [58,59]. It is composed of 1.8 million nodes and has a minimum resolution of 14 m in the Bay regions. The mesh is designed to study the storm surge impacts on the FEMA Region III areas, such as Washington DC, Maryland, Virginia, and thus, it has finer resolution in the Chesapeake Bay areas. The model domain extends from 60° W in the Atlantic Ocean to the 15 m contour line in the Mid-Atlantic coastal regions of the US. Figure 3 shows the model domain with selected storm tracks. The open ocean boundary of the model is forced by harmonic tides extracted from the Le Provost tidal database [60].

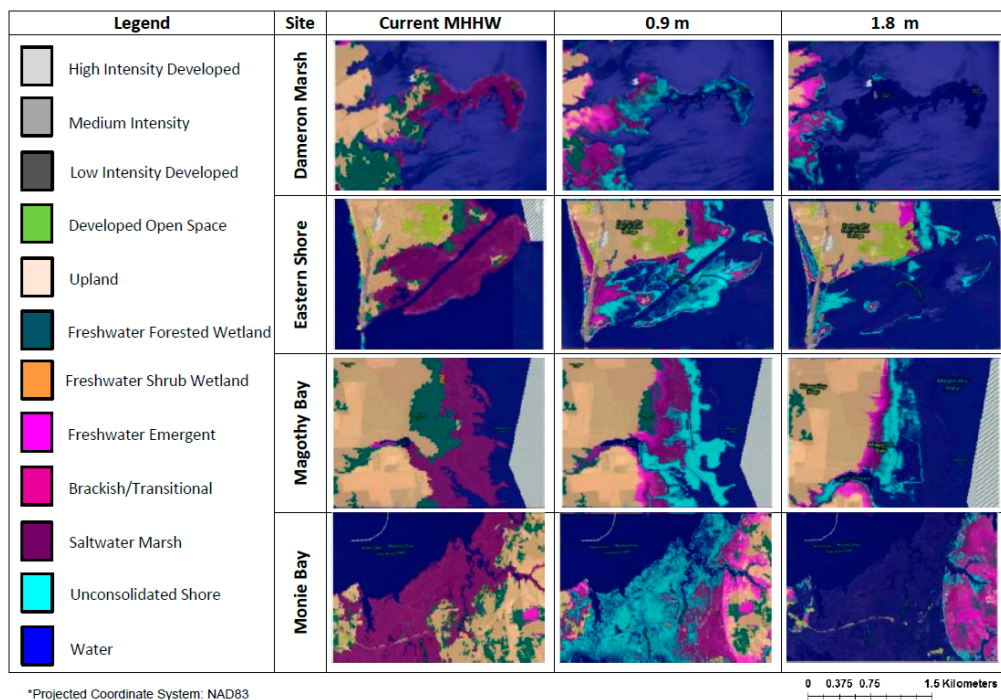


Figure 2. Land cover changes in each study area due to the different SLR-marsh migration scenarios.

Based on track locations and intensity three storms are selected to simulate the impacts of storm surge in coastal protected areas in the Chesapeake Bay. One recent historical storm, Irene (2011), and two synthetic storms (#35 and #145) developed under the North Atlantic Coast Comprehensive Study (NACCS) [61] are selected for this study. Based on statistical analysis of meteorological data and past historical storms tracks in the Mid-Atlantic region, NACCS generated symmetric synthetic storms for the Chesapeake Bay region [61]. The Synthetic145 storm travels parallel to the west side of the Bay, while the Synthetic35 cyclone travels through the Bay, crossing its main axis (Figure 3). Additionally, Hurricane Irene travels to the east of the Bay. In terms of storm intensity and forward speed, the selected storms represent a low to high strength hurricanes, including one of the major historical hurricanes, Irene that impacted the study area. Table 3 provides the minimum central pressure, maximum sustained wind speed and forward speed of the selected storms.

The storm parameters for Irene are collected from the National Hurricane Center (NHC) Hurricane Data 2nd generation (HURDAT2) database. To compute the meteorological forcing due to Hurricane Irene, ADCIRC uses the asymmetric vortex formulation [62,63] based on the Holland wind model [64], which generates the wind and pressure fields for each computational node in the model domain. Since the NACCS generated synthetic storms have symmetric wind field, the meteorological forcings for Synthetic35 and Synthetic145 storms in ADCIRC are calculated using the symmetric vortex formulation of the Holland Model [64]. Additionally, the wind stress over the free water surface is computed from the wind velocity using Garratt’s drag formulation [24].

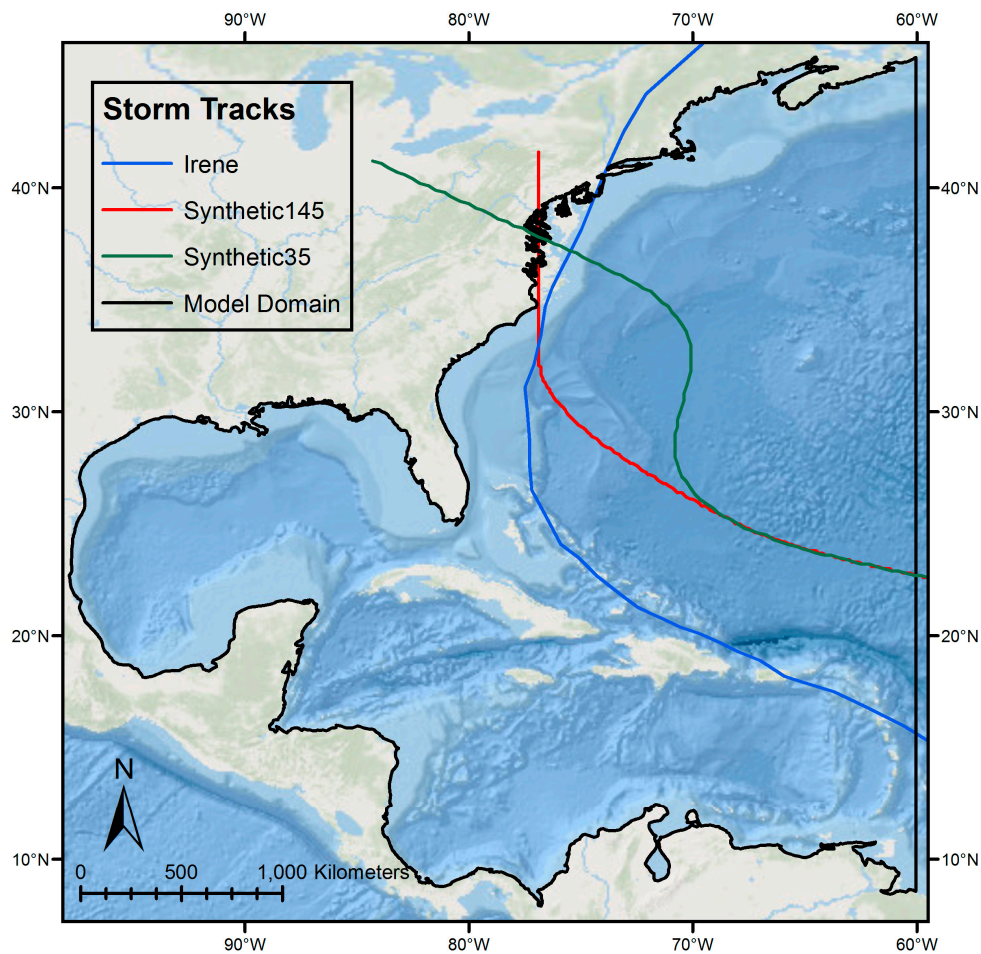


Figure 3. Numerical model domain and selected storm tracks.

Table 3. Wind and pressure intensity of the selected storms.

Storm	Min. Central Pressure (mb)	Max. Wind Speed (kt)	Forward Speed (m/s)
Hurricane Irene	942	105	8.76
Synthetic145	945	111	3.1
Synthetic35	985	64	9.18

The R3 mesh used in this study was calibrated and validated for multiple historical storms during the model development phase [58]. For this study, the model performance is estimated for Hurricane Irene by comparing the simulated peak water levels with observed maximum water levels at NOAA tidal stations located within the Chesapeake Bay areas. The model performance—difference between observed and modeled maximum water elevation—at most of the NOAA tide station locations across the Bay areas showed an overall variance or error (model minus observed) of 0.5 m. For example, the closest NOAA stations to Dameron Marsh and Monie Bay have approximate 0.1 m and -0.05 m errors, respectively (Figure A1: Appendix A). The averaged observed tidal range at the NOAA stations can vary from 0.9 m to 1.3 m [46,65–67]. For Eastern Shore and Magothy Bay, the error at the nearest observed locations are about 0.2 m. Thus, in the selected protected areas, the model performance can vary within a range of 0.2 m to 0.05 m. Although there are some differences in the modeled and observed peak water levels at some of the locations, the results are satisfactory for this study.

2.5. Preserve Areas and Sea Level Rise in the Model

The hydrodynamic and waves regimes in the preserve areas for the selected storms are calculated based on current conditions (i.e., without rise in sea level and using the existing land use information). The analysis is repeated considering the future scenarios incorporating the projected local SLR and potential land use change due to marsh migration. SLR is directly included in the models using eustatic method [29,31,68,69], in which mean sea water level is offset by the locally projected SLR values. Different land use and land cover is represented in the model through frictional drag coefficient (Manning's N) as bottom shear stress. Additionally, the dissipation of momentum transfer from wind to the water column by vegetation in the wetlands and marshes are delineated using surface canopy and land roughness length. Details about the land cover inclusion in ADCIRC is provided in Atkinson et al. [70] and Ferreira et al. [71]. The frictional parameters are assigned on each computational node of the mesh for different land cover types taken from C-CAP database. C-CAP divides wetlands and marshes as palustrine and estuarine categories where each category is subdivided into forested, shrub and emergent wetlands. Note that the frictional coefficients will change depending on the SLR and marsh migration scenarios according to the land cover type changes within the preserves. The frictional parameters in the storm surge model for each land cover types including wetlands and marshes are provided in Table A1. In addition, the average model mesh resolution within the selected preserve areas is approximately 200 m. Thus, the projected marsh migration in the preserve areas are represented in the model in a coarse scale.

Simulated maximum water level, maximum wave height, and maximum velocities for each storm and scenario were incorporated in ArcGIS using the Arc Storm Surge tool [72]. The hydrodynamic and waves regime is analyzed within each preserve area boundary. For calculating the hydrodynamic and wave responses in the study sites, each variable, such as maximum water level or wave heights, are averaged across all the numerical mesh nodes within the protected land boundaries.

3. Results

3.1. Impacts of Sea-Level Rise on Flooding Extent

In order to estimate the flooding extent in the protected areas, the percentage-flooded area due to the selected storms is plotted in Figure 4. The plot for each site shows the percent of inundated area due to storm surge for the current condition and different SLR scenarios. The zero SLR value in the *x*-axis of the plots represents the current condition.

As expected, the results show that SLR and land use change due to marsh migration will increase the inundation in all of the preserve areas. Figure 4 also shows that the percent flooded area for both current condition and the future SLR scenarios varies for each study sites. In addition, increase in flooded area substantially varied due to different rates of SLR. For example, depending on the storm intensity and location, in current condition, 7–10% of the land area of the Dameron Marsh is inundated due to storm surge, which rises up to inundating the entire reserve (100% inundation) with the “highest” SLR scenario regardless of the storm. On the other hand, in Monie Bay, regardless of SLR, the entire preserve area experienced storm surge inundation even under current conditions. The scenario is different for the Magothy Bay and Eastern Shore, which are located at the tip of the Chesapeake Bay. The results show a gradual increase in storm surge flooded areas due to SLR for both Eastern Shore and Magothy Bay preserve areas. None of the two preserve areas are expected to have a 100% flooded area for any storm, even with the highest rate of SLR. However, all preserve areas, except Eastern Shore, are likely to have more than 70% of the total area to be flooded with the highest SLR. Additionally, as expected for most of the cases, the storm intensity played an important role in storm surge inundation in the coastal protected areas. For instance, Hurricane Irene, which is the strongest of the selected storms, caused more coastal flooding than the Synthetic storms in the protected areas. The detailed percent of inundated area for the selected storms and protected areas are provided in Table A2.

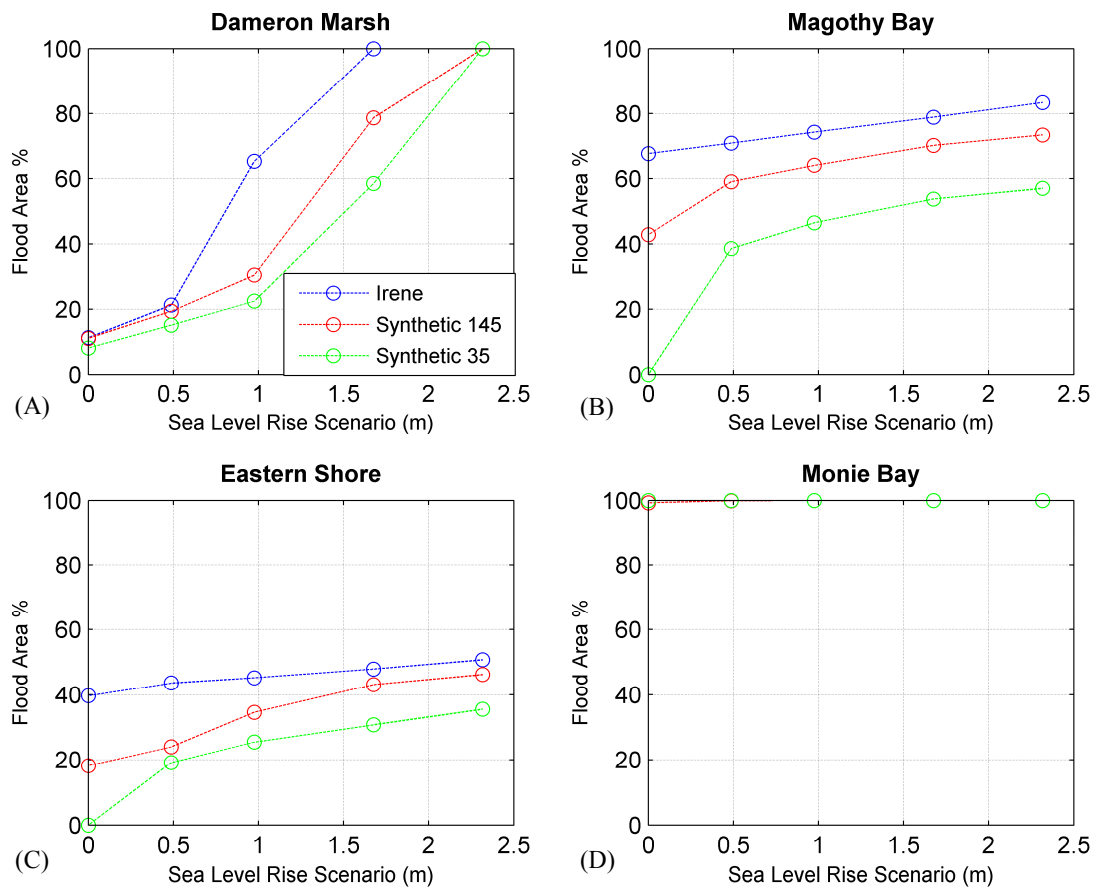


Figure 4. Percent of inundated area at each preserve areas for current condition and different SLR scenarios. The top panel shows the percent of inundated area for (A) Dameron Marsh and (B) Magothy Bay. In the bottom panel results are shown for (C) Eastern Shore and (D) Monie Bay Preserve Area.

3.2. Impact of Sea-Level Rise on Maximum Water Levels

In addition to increase in flooded extent, the results show an increase in surge induced maximum water levels in the preserve areas due to SLR. Similar to the Figure 5, the maximum water levels due to the selected storms are plotted in Figure 5, for each of the preserve areas for current conditions and future SLR scenarios.

The plots in Figure 5 clearly show that for both current and future conditions, Hurricane Irene has higher impact on maximum water levels than the other two storms. Although the maximum water levels in each of the preserve areas are distinct for different SLR scenarios, in general, the “highest” inundation height in the protected areas can rise up to 3.5 to 4.6 m, which is almost 1.5 to 2.5 m higher than the flood elevation in the current day storm surge flooding. The results also suggest that increase in water elevation tends to have a linear relationship with the increase in SLR. For example, observing the impact of Irene in Dameron Marsh, a SLR of 0.48 m raises the storm surge water level to 1.84 m. This is 0.42 m greater than the No SLR case, which is almost equal to the amount of SLR that was introduced into the system. Similar patterns are also observed in rest of the preserve areas. In terms of the maximum rise in water level, the Eastern shore and Magothy Bay preserve areas are likely to have higher surge induced flood elevation for both current condition and SLR scenarios than Dameron Marsh and Monie Bay. This could be due to the location of the preserve areas as both Eastern shore and Magothy Bay are situated in the mouth of the Bay and closest to the open ocean. Detailed maximum elevation values for the selected storms and scenarios for all protected lands are provided in Table A3.

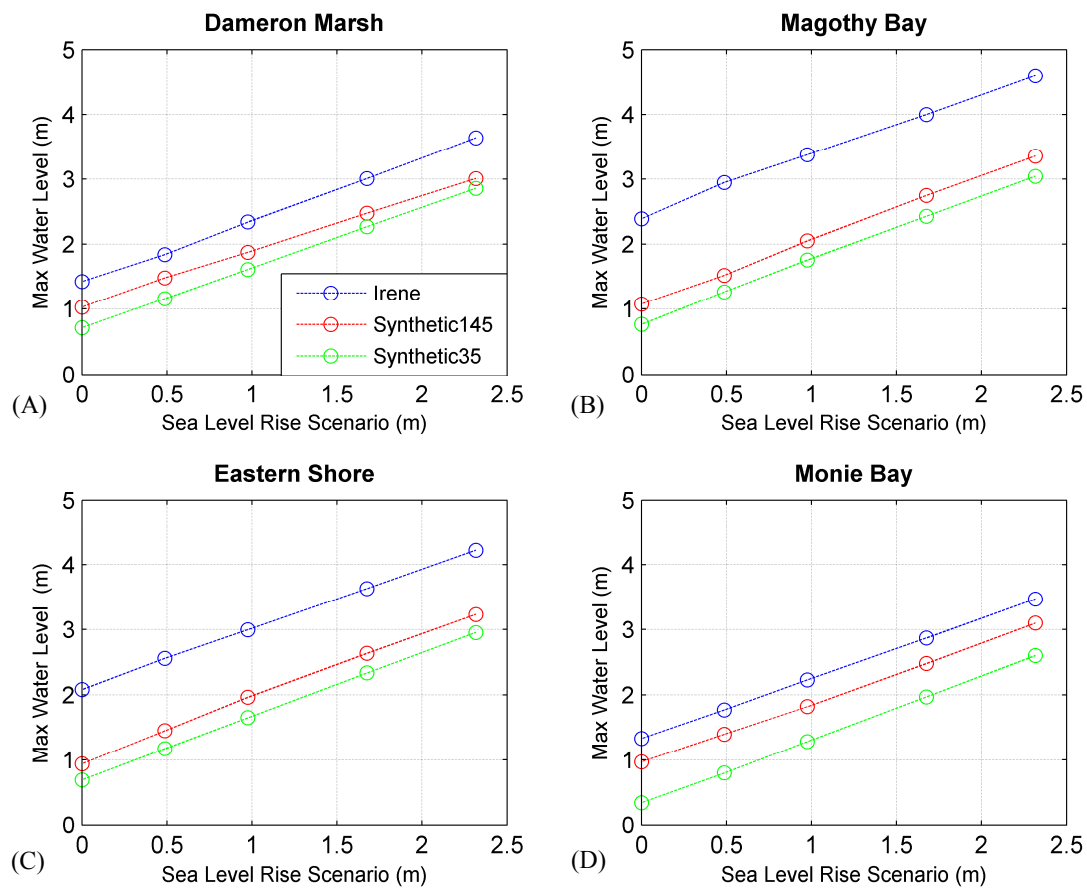


Figure 5. Maximum water levels at each preserve areas for current condition and different SLR scenarios. The top panel shows the simulated maximum water level in (A) Dameron Marsh and (B) Magothy Bay. In the bottom panel results are shown for (C) Eastern Shore and (D) Monie Bay Preserve Area.

3.3. Impact of Sea-Level Rise on Currents Velocities

In order to investigate flood propagation, erosion and potential vegetation damage in the protected areas, the study calculated the maximum current velocities in all preserve areas for the simulated storms. Figure 6 provides the maximum current velocities due to selected storms at each of the study sites for present-day condition and for the SLR projections.

The results suggest that the impacts of both storm surge and sea-level rise on currents in the protected areas are highly site specific, although a higher rate of SLR notably increases the current velocity at each preserve area. For example, depending on the storm intensity and track, the maximum current velocities in Monie Bay can reach up to a maximal of 0.35 m/s in the ‘highest’ SLR scenario. While for both Dameron Marsh and Eastern Shore, the “highest” maximum current velocities are higher than 1 m/s. Figure 6 also shows that current velocities are more sensitive to SLR in Dameron marsh and Eastern Shore than Monie Bay and Magothy Bay. Though both Magothy Bay and Eastern Shore are located close to the mouth of the Chesapeake Bay, Magothy Bay experiences significant lower current energy due to the protection from the surroundings Mockhorn Island and Smith Island. Similarly, Monie Bay is located in the mid Bay, confined by landmasses and exposed to relatively lower energy during hurricanes when compared to the other preserves. Maximum velocities substantially varied with different SLR scenarios for each preserve areas, presenting a non-linear response to SLR. For example, with a 0.49 m rise in sea-level, the maximum velocities in the Dameron Marsh and Magothy Bay decrease from the current condition, while Monie Bay shows increases from the baseline. However, with higher increase in SLR, regardless of the storms, all the preserve areas

showed considerable increase in maximum currents velocities. Furthermore, the results show that hurricane Irene has higher impacts on currents velocities in the preserve areas than the Synthetic storms for both current condition and SLR scenarios. The only exception is at Dameron Marsh, where the impact of Synthetic Storm 145 is always higher than both Irene and Synthetic Storm 35. This indicates the significance of the location respect to the storm track on maximum current velocities in the protected areas. While Hurricane Irene travelled parallel to the east of the Bay, both Synthetic storms passed through the mid Bay region near the Dameron Marsh (Figure 3). Contrarily, the wind intensity of Synthetic35 is almost the half of the wind intensity of Synthetic145 and Irene. Therefore, in Dameron Marsh, Synthetic145 has the highest impacts on currents velocities than the other two storms. The detailed currents velocity values in all protected areas for the selected storms and scenarios are provided in Table A4.

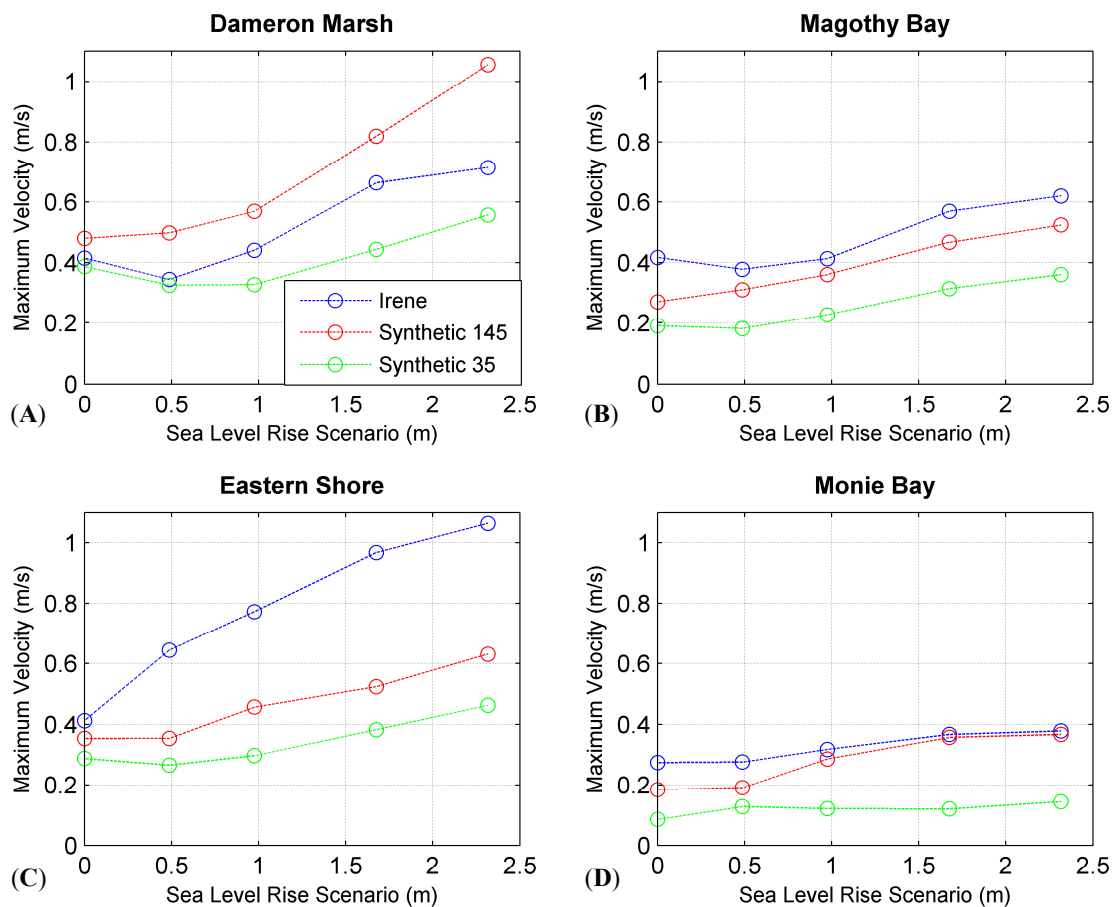


Figure 6. Maximum currents velocities at each preserve areas for current condition and different SLR scenarios. The top panel shows the simulated maximum currents velocity in (A) Dameron Marsh and (B) Magothy Bay. In the bottom panel results are shown for (C) Eastern Shore and (D) Monie Bay Preserve Area.

3.4. Impact of Sea-Level Rise on Wave Heights

In Figure 7, the maximum wave heights at each of the preserve areas are shown for current and future SLR scenarios. In terms of change in wave heights in the preserve areas, the results show an increase due to the rise in sea-level. Figure 7 shows that the impacts of wave heights in all preserve areas are higher for Hurricane Irene, which as expected, indicates that higher storm intensity will have higher impacts on wave heights in the protected areas.

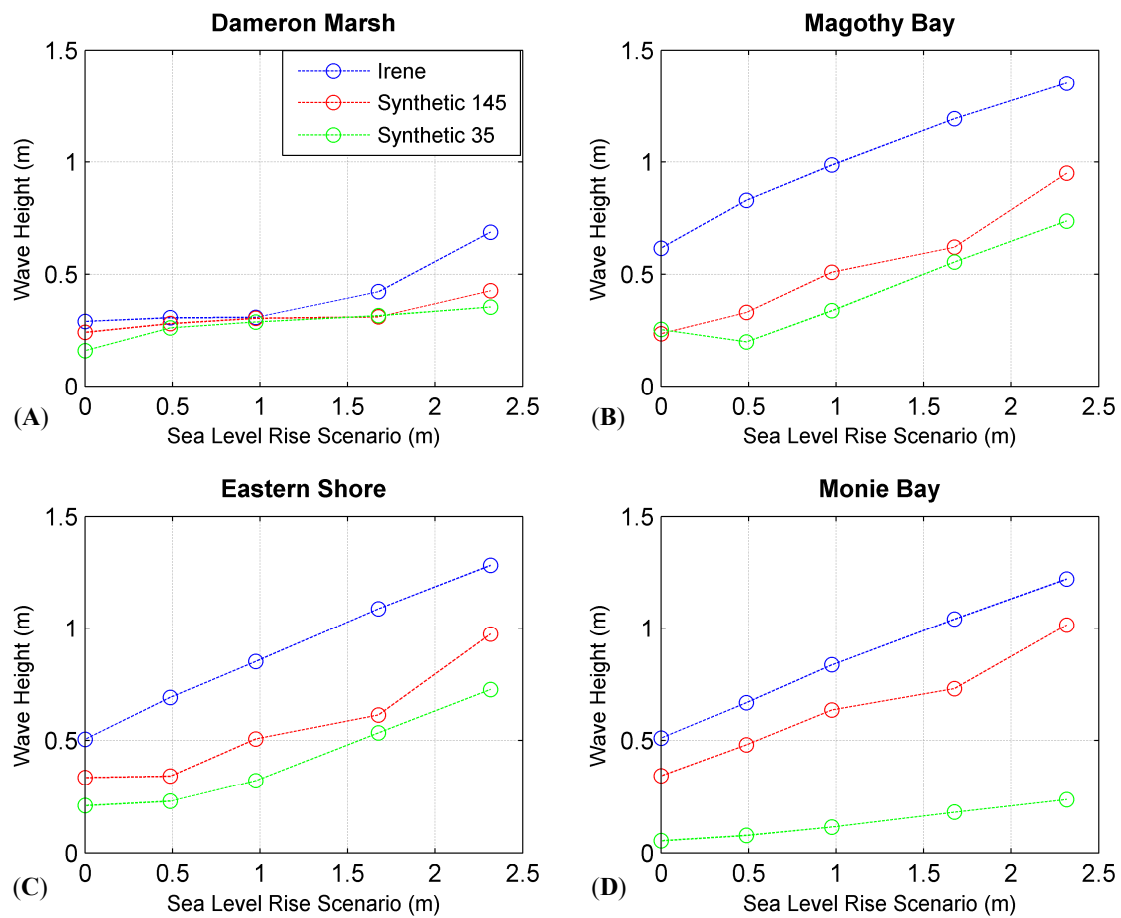


Figure 7. Maximum wave heights at each preserve areas for current condition and different SLR scenarios. The top panel shows the simulated maximum wave heights in (A) Dameron Marsh and (B) Magothy Bay. In the bottom panel results are shown for (C) Eastern Shore and (D) Monie Bay Preserve Area.

Furthermore, except for Dameron Marsh, SLR significantly increases the wave heights in the preserve areas. For instance, in Eastern Shore and Magothy Bay, a 0.97 m of SLR during hurricane Irene increases the maximum wave heights by 0.5 m, which is almost a 100% increase from the current conditions. For Dameron Marsh, until the “highest” scenario, no significant increase in wave heights is found with SLR. However, in the rest of the preserve areas, the current wave heights due to storm surge are considerably higher than Dameron Marsh. This indicates that preserve areas with higher wave heights without any SLR will have higher rate of increase due to SLR than the ones with lower wave impacts currently. Additionally, the “highest” SLR scenario leads to more than 100% increase in maximum wave heights from the current conditions during any storm events. For example, depending on the storms, a 2.3 m of SLR can increase the maximum wave heights in Monie Bay from a range of 0.05–0.5 m to 0.25–1.2 m. Detailed wave heights in the protected areas for the selected storms and scenarios are provided in Table A5.

4. Discussion and Implications

The results showed that the hydrodynamic responses inside the preserve area to storm surge, SLR, and marsh migration are site-specific. Therefore, in this section, the findings are summarized to contextualize the results for a regional scale and provide an overall understanding on the impacts of our results in coastal protected areas. Our results indicate that storm intensity plays a significant role in inundation, maximum water levels, and wave heights in the protected areas. The highest intensity

storm, Irene, showed higher impacts on the study sites. Figure 8 shows the inundation area and the maximum water levels under different rates of SLR for hurricane Irene in the four preserve areas. The inundation maps in Figure 8 also indicates that the “highest” SLR can raise inundation height in the protected areas to an average of 3.5 to 5 m which is almost 1.5 to 2.5 m higher than the current day flood elevation. The study by Xia et al. (2008) [73] also found out the significance of storm track and intensity in storm surge inundation.

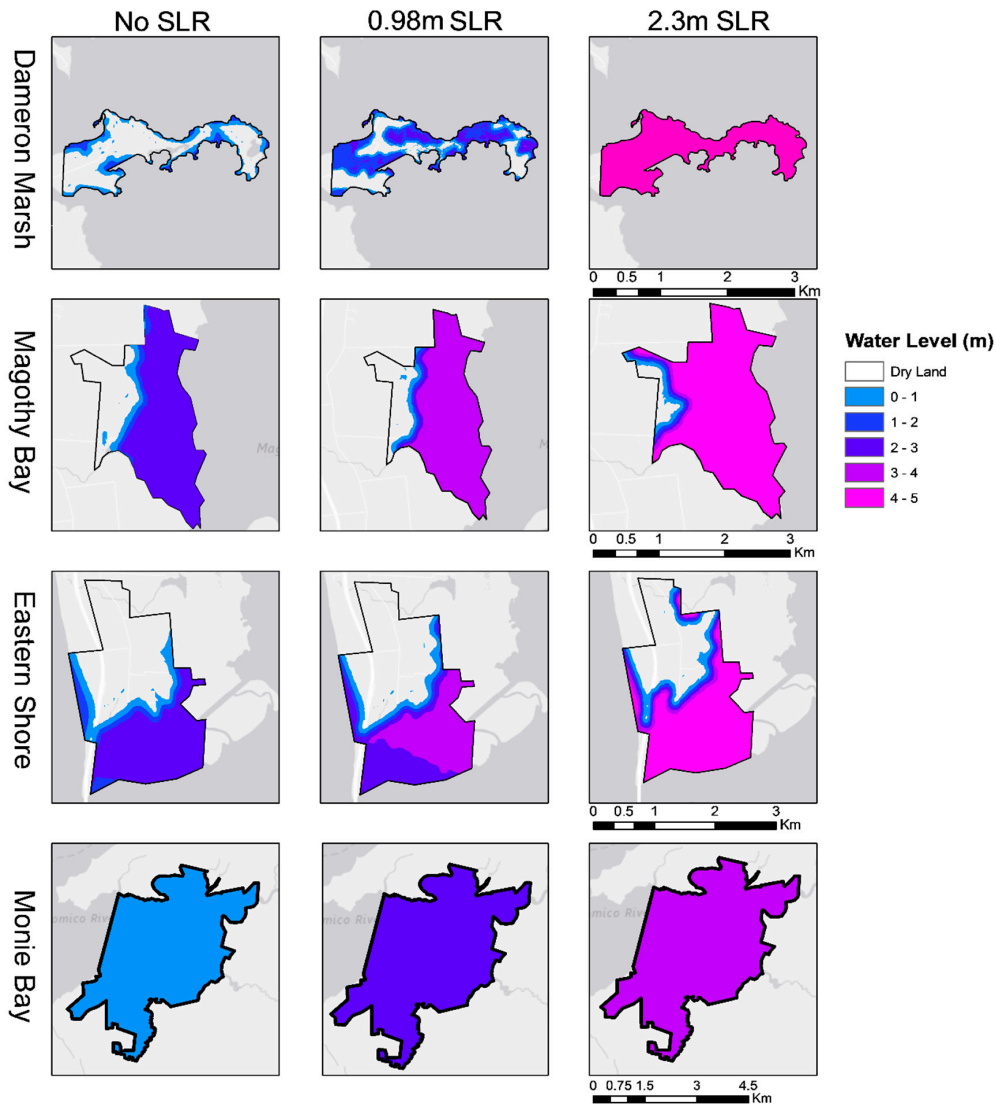


Figure 8. Current and future SLR scenario Inundation maps for the selected preserve areas in the Chesapeake Bay.

Figures 8 and 9 show that, regardless of the storm, almost 100% of Monie Bay land area is inundated by storm surge. In terms of increase in flood extent, results indicate that Dameron Marsh is the most sensitive preserve area to SLR. The average percent of storm surge flooded area in Dameron Marsh increases rapidly, as the rate of SLR increases while for Magothy Bay and Eastern Shore the flooded area gradually expands with the increases in SLR. This reflects the uniqueness of the coastal protected areas in terms of their location and topography. For example, the nearshore elevation at both Eastern Shore and Magothy Bay are around 0–2 m which rises up to an average 2–5 m in areas further inland. Therefore, even in the “highest” SLR scenario with an average maximum water elevation of 3–3.5 m, both preserve areas are not entirely inundated (Figure 8). In contrast, Dameron Marsh

and Monie Bay have a relatively flat and constant slope, ranging between 0–2 m within the preserve areas. Thus, a “maximum” of 3 m height of flooding inundates the entire preserve areas. This higher exposure to coastal flooding in these preserve areas can consequently reduce the plant growth and organic matter input that decreases with excess inundation [20]. Our findings suggest that the increase in flooding extent inside the preserves is not linearly related to SLR. A study by Li et al. [74] (2012) in Norfolk, Virginia, also found a nonlinear relationship where a 50-year storm with 1 and 2 m SLR increased total inundated area 34% and 69%, respectively, that changed to 74% and 78% when analyzed for a 100-year storm for same SLR rates. Another study in the Galveston Bay and Jefferson County, Texas, found that the SLR and changing landscapes inundated three times more land when increasing from 0.402 m to 0.926 m [15]. However, the results demonstrated a linear relationship between surge induced water elevation in the protected areas with SLR. These results differ from Bilskie et al. [13], where for coastal areas in Alabama and Mississippi, they found that the increase in water levels was greater than the amount of water added due to SLR. It should be noted, that the focus of our study is on four coastal preserve areas that are spatially very small in compared to the coastal areas studied by Bilskie et al. [13]. These findings suggest that the preserves sizes are not large enough to allow for a fully developed interaction between storm surge hydrodynamics and friction; thus, the long wave associated to the storm surge is not significantly affected within these spatial scales, as observed by Bilskie et al. [13] in the much larger marshes of the Louisiana coast.

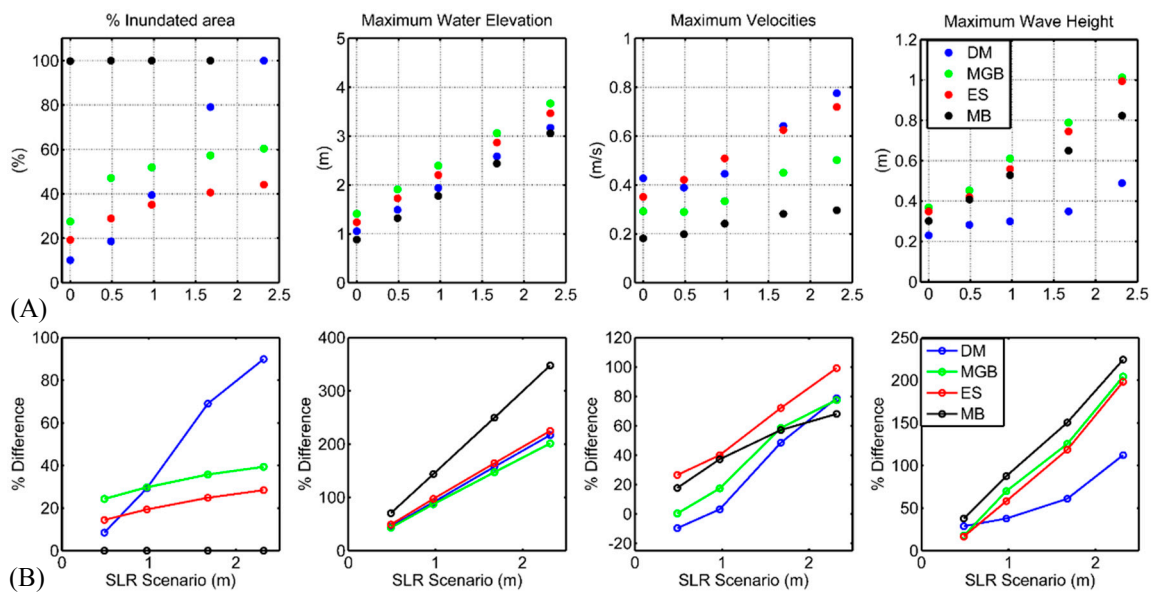


Figure 9. Overall impacts of SLR and marsh migration on Percentage of inundated area, maximum water levels, maximum currents and maximum wave heights at each preserve area. The top panel (A) shows the average of the simulated Percentage of inundated area, maximum water levels, maximum currents and maximum wave heights for the selected storms in both current and future scenarios while in the bottom panel (B) percentage increase of each of the parameters from the current condition are shown for the selected sites.

When compared with the current conditions, our results show that a maximum of 2.3 m rise in SLR can amplify the current maximum flood elevation in the protected areas by about 200%. This overall increase in maximum water elevation can largely affect the existing vegetation in coastal protected areas in Chesapeake Bay region. For current velocities, the increase is relatively small until 0.97 m of SLR, which significantly amplifies with a higher rate of SLR projections such as 1.68 m and 2.31 m. This implies that a higher rate of SLR can intensify the nearshore erosion in the coastal marshes in the preserve areas, though no linear relationship is found between SLR and current velocities in protected

areas. Therefore, with increasing SLR, projected marsh migration and loss of wetlands, the potential shoreline erosion in the coastal protected areas are to likely intensify in future. Moreover, SLR has a significant effect on wave heights, where higher flood depths allow higher waves to propagate through the study area. Except at one site, Dameron Marsh, the increment in SLR showed an almost linear relationship with the increase in wave height in the preserve areas. A few recent studies [16,75] found a nonlinear trend between SLR and wave heights, although their focuses were not on the coastal protected areas. In terms of percent increase from current conditions, a 0.49 m of SLR increases maximum wave heights in the protected areas by less than 50% and a 2.3 m of SLR amplifies by more than 200%. The projected increase in wave heights and water levels in the protected areas can substantially affect the ecosystem service provided by the protected areas. For example, two recent studies [46,76] in the Chesapeake Bay regions applied observed field data in our study site to evaluate the surge and wave attenuation by coastal marshes. Both studies showed that marshes' capacity to attenuate surge and wave heights decreases with increasing inundation and water level. Thus, increase in inundation, water level, and wave heights in the preserve areas due to SLR and marsh migration will lower protected areas capacity to reduce surge level and wave heights, and provide flood protection service.

While the lower rates of sea level could result in adjustable hydrodynamic changes in the study sites, a higher increase of sea level has the potential to significantly alter the hydrodynamic responses to surge and waves and the hydrologic regime within the protected areas. Our results indicate that, for the coastal preserve areas in Chesapeake Bay, considerable increase in the hydrodynamics and waves is observed when SLR exceeds by 1 m. The increasing sea level will affect the distribution of salt marshes [77], and the losses of the saline wetlands are happening at a fast rate [8]. Our study indicates that, with storm surge, the inundation scenario will intensify in coastal wetlands and marshes. This implies that the sustainability of the marshes and wetlands in the protected areas are at a higher risk in the future. Larger currents and wave heights that are caused by the effects of SLR and storm surge might lead to increased coastal erosion. Higher current velocities and wave heights will transport more energy and momentum to the shore, which can cause a faster rate of erosion in the nearshore areas [78]. Therefore, results of the study can provide an improved understanding of the risks associated with SLR to support future management actions, policy, and practices to preserve the coastal protected areas. In addition, incorporating marsh migration in modeling future flooding can add further insights on how sea level can affect the coastal protected areas in the US. The methods applied in this study can also be implemented for other low-lying natural reserves in the coastal areas that are vulnerable to SLR and storm surge.

Though all sites showed higher flooding, each site revealed distinct responses to SLR in terms of faster intrusion of seawater and waves. This indicates two important implications in understanding the vulnerability of the coastal marshes in the protected areas. First, for improved interpretation of how the marshes and wetlands in the protected areas will respond to SLR, local scale analysis is required, since marsh dynamics are highly site specific. Second, the incorporation of marsh migration scenarios is essential when assessing the impacts of SLR on coastal protected areas.

5. Conclusions

Coastal protected areas serve as natural habitats to multiple ecosystems and offer a range of services from flood protection to recreation. Most of the coastal protected areas contain wetlands and marshes, which are unique in nature and are exposed to flooding due to storm surge and SLR. In this study, we combined the impacts of SLR, marsh migration and storm surge on four preserve areas located in different parts of the Chesapeake Bay to assess how coastal hydrodynamics and waves within the protected areas are likely to change in the future. Coupled surge and wave simulations are implemented to gain an improved understanding of the coastal inundation impacts to the Chesapeake Bay preserve areas. We included historical and synthetic storms in our simulations to capture a spectrum of storms and their impacts in the study areas. The simulations incorporated four different

local SLR projections based on the National Climate Assessment and regional land subsidence rate. Potential land use changes due to SLR driven marsh migration are also included in our analysis to provide a more accurate representation of future land cover in the protected areas.

Comparing current and projected future inundation extent, maximum flood elevation, current velocity, and waves in four preserve areas in the Chesapeake Bay showed that SLR will increase the hydrodynamics and waves impacts in coastal protected areas. Our study indicates that protected areas responses to both storm surge and SLR are highly site-specific and depend on location, topography, and coastal features of the preserve areas. Therefore, adaptation strategies and restoration plans for the coastal protected areas should be site specific. In terms of the selected sites in the Chesapeake Bay, Monie Bay is found to be the most vulnerable preserve area to coastal flooding, while Dameron Marsh appears to be most sensitive site to SLR. Results also demonstrated that the hydrodynamic and wave responses of the protected areas significantly depend on storm intensity, track and proximity to the shore. Furthermore, findings on the preserve areas in the Chesapeake Bay suggest a linear relationship between SLR and surge induced water elevation in the protected areas. Moreover, the impacts of SLR were significantly greater after a 1 m threshold of SLR, suggesting the presence of a critical limit for conservation strategies.

The projected increase in the hydrodynamic and wave impacts on the preserves can affect the hydrologic regime, salinity, and local geomorphology in coastal protected areas. Higher increase in inundation and potential shoreline erosion can consequently change the ecology of the wetlands and marsh in these natural reserves. While the eco-morphological consequences in the protected areas due to storm surge and SLR are not investigated in this study, the results from the regional scale storm surge and wave models can be applied in local scale hydro-morphodynamic model to quantify marshes vulnerability to SLR and to advance the understanding of the projected ecological changes in coastal protected areas. It is worth mentioning that fine scale site-specific morphodynamic and eco-biological data are required to address the vulnerability of tidal wetlands and distribution of marshes due to SLR. Thus, our findings derived from the coarse scale representation of marsh migration should be qualitatively taken into account at best. Additionally, model parameterization needs improvement in representing the interaction between marsh vegetation and storm hydro- and wave dynamics. However, in this study, we provide a suitable method to estimate the potential changes in hydrodynamics and waves in coastal protected areas for storm surge, SLR, and marsh migration that may help to develop necessary adaptation plans for the long-term sustainability of coastal protected areas.

Author Contributions: The paper was conceived and designed by A.M.R., C.M.F., A.B., and J.L.G., A.B. has carried out the simulations, pre- and post-processed the results under the supervision of J.L.G., A.M.R., and C.M.F. Finally, results analysis, interpretation and manuscript preparation are carried out by all authors.

Funding: This research received no external funding.

Acknowledgments: This material is based upon work supported by the National Science Foundation under Grant No. SES-1331399. Any opinions, findings, and conclusions or recommendations expressed in this material are those of the authors and do not necessarily reflect the views of the National Science Foundation. This material is also based upon work supported by the National Fish and Wildlife Foundation and the U.S. Department of the Interior under Grant No. 43932. The views and conclusions contained in this document are those of the authors and should not be interpreted as representing the opinions or policies of the U.S. Government or the National Fish and Wildlife Foundation and its funding sources. Mention of trade names or commercial products does not constitute their endorsement by the U.S. Government, or the National Fish and Wildlife Foundation or its funding sources. Additionally, this research work was partially supported by Virginia Sea Grant Program Development funding (Project Number: R/71851B-PD) and the authors would like to thank Virginia Sea Grant for funding the open access publication of the manuscript. This work used the Extreme Science and Engineering Discovery Environment (XSEDE), which is supported by National Science Foundation grant number ACI-1053575. The authors would like to express sincere gratitude to NOAA Digital coast for providing the land cover projection data. The authors acknowledge the Texas Advanced Computing Center (TACC) at the University of Texas at Austin for providing HPC resources that have contributed to the research results reported within this paper (<http://www.tacc.utexas.edu>).

Conflicts of Interest: The authors declare no conflict of interest.

Appendix A

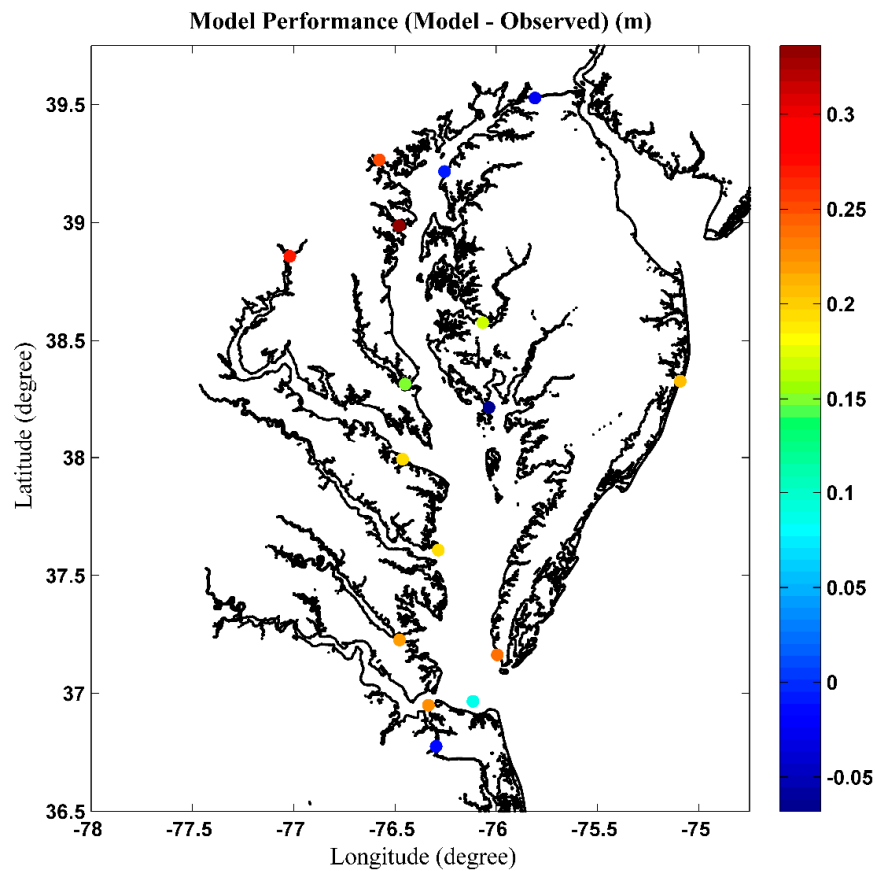


Figure A1. Model validation for Irene showing the error in maximum water level.

Table A1. Frictional parameter values applied in the storm surge and waves model.

Land Cover Type	Class Number	Manning's N	Surface Canopy Coefficient	Surface Directional Effective Roughness Length
Unclassified	1	0	1	0
Developed, High Intensity	2	0.12	1	0.3
Developed, Medium Intensity	3	0.12	1	0.3
Developed, Low Intensity	4	0.07	1	0.3
Developed, Open Space	5	0.035	1	0.3
Cultivated Crops	6	0.1	1	0.06
Pasture/Hay	7	0.055	1	0.06
Grassland/Herbaceous	8	0.035	1	0.04
Deciduous Forest	9	0.16	0	0.65
Evergreen Forest	10	0.18	0	0.72
Mixed Forest	11	0.17	0	0.71
Scrub/Shrub	12	0.08	1	0.12
Palustrine Forested Wetlands	13	0.2	0	0.6
Palustrine Scrub/Shrub Wetlands	14	0.075	1	0.11
Palustrine Emergent Wetlands	15	0.07	1	0.3
Estuarine Forested Wetlands	16	0.15	0	0.55
Estuarine Scrub/Shrub Wetlands	17	0.07	1	0.12
Estuarine Emergent Wetlands	18	0.05	1	0.3
Unconsolidated Shore	19	0.03	1	0.09
Barren Land	20	0.03	1	0.05
Open Water	21	0.025	1	0.001
Palustrine Aquatic Bed	22	0.035	1	0.04
Estuarine Aquatic Bed	23	0.03	1	0.04

Table A2. The percent of inundated land area for each marsh and the percent increase in flooded area shown in parenthesis.

Irene					
Preserve Area	No SLR	0.48 m	0.97 m	1.68 m	2.31 m
DM	11.3	21.3 (10%)	65.3 (54%)	100 (88.7%)	100 (88.7%)
MGB	67.7	70.9 (3.2%)	74.3 (6.7%)	78.9 (11.3%)	83.4 (15.7%)
ES	39.7	42.6 (2.9%)	45.2 (5.5%)	47.9 (8.2%)	50.7 (11%)
MB	100	100 (0%)	100 (0%)	100 (0%)	100 (0%)
Synthetic 145					
-	No SLR	0.48 m	0.97 m	1.68 m	2.31 m
DM	11.1	19.4 (8.3%)	30.5 (19.4%)	78.7 (67.7%)	100 (88.9%)
MGB	42.8	59.1 (16.3%)	64.1 (21.3%)	70.2 (27.4%)	73.4 (30.6%)
ES	18.2	24.0 (5.8%)	34.6 (16.4%)	43.1 (24.9%)	46.2 (28%)
MB	99.3	99.9 (0.6%)	100 (0.7%)	100 (0.7%)	100 (0.7%)
Synthetic35					
-	No SLR	0.48 m	0.97 m	1.68 m	2.31 m
DM	8.08	15.2 (7.09%)	22.5 (14.4%)	58.6 (50.5%)	100 (91.9%)
MGB	14.6	53.2 (38.6%)	61.1 (46.5%)	68.4 (53.8%)	71.7 (57%)
ES	10.5	29.7 (19.1%)	36 (25.5%)	41.3 (30.8%)	46.1 (35.5%)
MB	100	100 (0%)	100 (0%)	100 (0%)	100 (0%)

Table A3. Modeled Data showing the maximum water levels for each Preserve Area. The percent increase in water level is shown in parenthesis.

Irene					
Preserve Area	No SLR	0.48 m	0.97 m	1.68 m	2.31 m
DM	1.42	1.84 (29.5%)	2.34 (65%)	3.02 (112.7%)	3.64 (156.3%)
MGB	2.39	2.95 (23.2%)	3.38 (41.4%)	4.01 (67.5%)	4.60 (92.3%)
ES	2.08	2.56 (22.9%)	3.00 (44.1%)	3.63 (74.3%)	4.22 (102.9%)
MB	1.33	1.77 (33.2%)	2.23 (67.9%)	2.87 (116.5%)	3.47 (161.7%)
Synthetic 145					
-	No SLR	0.48 m	0.97 m	1.68 m	2.31 m
DM	1.03	1.48 (43.7%)	1.87 (82.3%)	2.48 (141.3%)	3.01 (193.2%)
MGB	1.07	1.52 (41.4%)	2.05 (90.8%)	2.75 (156.1%)	3.36 (212.7%)
ES	0.94	1.45 (54.1%)	1.96 (108.8%)	2.64 (180.4%)	3.23 (243.9%)
MB	0.97	1.4 (43.2%)	1.8 (86.7%)	2.5 (154.8%)	3.1 (218.2%)
Synthetic35					
-	No SLR	0.48 m	0.97 m	1.68 m	2.31 m
DM	0.71	1.16 (62%)	1.61 (125.5%)	2.27 (217.9%)	2.86 (301%)
MGB	0.76	1.26 (65%)	1.75 (129.4%)	2.43 (217.7%)	3.05 (298.3%)
ES	0.69	1.17 (69.5%)	1.65 (138.4%)	2.34 (237.5%)	2.95 (326.9%)
MB	0.34	0.80 (134.1%)	1.28 (275.7%)	1.97 (476.7%)	2.60 (662.2%)

Table A4. Modeled data showing the maximum currents velocities for each Preserve Area. The percent increase in maximum currents velocities is shown in parenthesis.

Irene					
Preserve Area	No SLR	0.48 m	0.97 m	1.68 m	2.31 m
DM	0.42	0.34 (-17.1%)	0.44 (6.1%)	0.66 (59.9%)	0.71 (72.2%)
MGB	0.42	0.38 (-9.3%)	0.41 (-0.89%)	0.57 (36.5%)	0.62 (48.8%)
ES	0.41	0.64 (56.4%)	0.77 (87.4%)	0.97 (134.9%)	1.06 (158.2%)
MB	0.27	0.28 (0.71%)	0.32 (15.9%)	0.37 (34%)	0.38 (38%)
Synthetic 145					
-	No SLR	0.48 m	0.97 m	1.68 m	2.31 m
DM	0.48	0.50 (3.8%)	0.57 (18.6%)	0.82 (70.6%)	1.06 (120%)
MGB	0.27	0.31 (15%)	0.36 (33.5%)	0.47 (73.8%)	0.52 (94.4%)
ES	0.35	0.46 (30.5%)	0.46 (29.1%)	0.52 (48.1%)	0.63 (78.3%)
MB	0.18	0.19 (3.53%)	0.29 (54.8%)	0.36 (93.4%)	0.37 (98.5%)
Synthetic35					
-	No SLR	0.48 m	0.97 m	1.68 m	2.31 m
DM	0.39	0.33 (-15.8%)	0.33 (-15.4%)	0.44 (14.62%)	0.56 (44%)
MGB	0.19	0.18 (-4.86%)	0.23 (19.4%)	0.31 (65%)	0.36 (89.4%)
ES	0.29	0.27 (-7.52%)	0.30 (3.36%)	0.38 (33.1%)	0.46 (60.8%)
MB	0.09	0.13 (48.7%)	0.12 (40.8%)	0.12 (39.9%)	0.14 (67.4%)

Table A5. Modeled data showing the maximum wave heights for each Preserve Area. The percent increase in wave heights is shown in parenthesis.

Irene					
Preserve Area	No SLR	0.48 m	0.97 m	1.68 m	2.31 m
DM	0.29	0.31 (5.79%)	0.31 (6.2%)	0.42 (45.6%)	0.69 (137.2%)
MGB	0.62	0.83 (34.6%)	0.99 (60.1%)	1.19 (93.6%)	1.35 (119.4%)
ES	0.50	0.69 (37%)	0.85 (68.7%)	1.09 (115.4%)	1.28 (153.7%)
MB	0.51	0.67 (30.9%)	0.84 (64%)	1.04 (104.1%)	1.22 (139.1%)
Synthetic 145					
-	No SLR	0.48 m	0.97 m	1.68 m	2.31 m
DM	0.24	0.28 (16%)	0.30 (26%)	0.31 (29%)	0.43 (76.8%)
MGB	0.24	0.33 (39.4%)	0.51 (116.1%)	0.62 (163.4%)	0.95 (303.2%)
ES	0.33	0.34 (3.1%)	0.51 (51.8%)	0.61 (84%)	0.97 (192%)
MB	0.34	0.48 (39.5%)	0.64 (86%)	0.73 (113.3%)	1.01 (197.2%)
Synthetic35					
-	No SLR	0.48 m	0.97 m	1.68 m	2.31 m
DM	0.16	0.26 (64%)	0.29 (80.6%)	0.32 (98%)	0.35 (122.2%)
MGB	0.25	0.20 (-21.6%)	0.34 (33%)	0.55 (118.4%)	0.74 (190.1%)
ES	0.21	0.23 (9.5%)	0.32 (53.5%)	0.53 (155.7%)	0.73 (248.1%)
MB	0.05	0.08 (42.6%)	0.11 (112%)	0.18 (233.2%)	0.24 (335.9%)

References

- Church, J.A.; Clark, P.U.; Cazenave, A.; Gregory, J.M.; Jevrejeva, S.; Levermann, A.; Merrifield, M.A.; Milne, G.A.; Nerem, R.; Nunn, P.D.; et al. Sea level change. In *Climate Change 2013: The Physical Science Basis. Contribution of Working Group I to the Fifth Assessment Report of the Intergovernmental Panel on Climate Change*; Cambridge University Press: Cambridge, UK; New York, NY, USA, 2013; pp. 1137–1216. [[CrossRef](#)]
- Church, J.A.; Gregory, J.M.; Huybrechts, P.; Kuhn, M.; Lambeck, C.; Nhuan, M.T.; Qin, D.; Woodworth, P.L. Changes in sea level. In *Climate Change 2001: The Scientific Basis: Contribution of Working Group I to the Third Assessment Report of the Intergovernmental Panel on Climate Change*; Houghton, J.T., Ding, Y., Griggs, D.J., Noguer, M., van der Linden, P.J., Dai, X., Maskell, K., Johnson, C.A., Eds.; Cambridge University Press: Cambridge, UK; New York, NY, USA, 2001; Chapter 11; pp. 639–694.
- Jevrejeva, S.; Moore, J.C.; Grinsted, A.; Woodworth, P.L. Recent global sea level acceleration started over 200 years ago? *Geophys. Res. Lett.* **2008**, *35*, 8–11. [[CrossRef](#)]
- Nerem, R.S.; Chambers, D.P.; Choe, C.; Mitchum, G.T. Estimating Mean Sea Level Change from the TOPEX and Jason Altimeter Missions. *Mar. Geod.* **2010**, *33*, 435–446. [[CrossRef](#)]
- IPCC. *Climate Change 2013: The Physical Science Basis. Contribution of Working Group I to the Fifth Assessment Report of the Intergovernmental Panel on Climate Change*; Cambridge University Press: New York, NY, USA, 2013; p. 1535. [[CrossRef](#)]
- Nicholls, R.J.; Cazenave, A. Sea Level Rise and Its Impact on Coastal Zones. *Science* **2010**, *328*, 1517–1520. [[CrossRef](#)] [[PubMed](#)]
- Blankespoor, B.; Dasgupta, S.; Laplante, B. *Sea-Level Rise and Coastal Wetlands Impacts and Costs*; Policy Research Working Paper; No. 6277; World Bank: Washington, DC, USA, 2012.
- Nicholls, R.J.; Hoozemans, F.M.J.; Marchand, M. Increasing flood risk and wetland losses due to global sea-level rise: Regional and global analyses. *Glob. Environ. Chang.* **1999**, *9*. [[CrossRef](#)]
- Nicholls, R.J. Coastal flooding and wetland loss in the 21st century: Changes under the SRES climate and socio-economic scenarios. *Glob. Environ. Chang.* **2004**, *14*, 69–86. [[CrossRef](#)]
- Knutson, T.R.; McBride, J.L.; Chan, J.; Emanuel, K.A.; Holland, G.; Landsea, C.; Held, I.; Kossin, J.P.; Srivastava, A.; Sugi, M. Tropical cyclones and climate change. *Nat. Geosci.* **2010**, *3*, 157–163. [[CrossRef](#)]
- Elsner, J.B.; Kossin, J.P.; Jagger, T.H. The increasing intensity of the strongest tropical cyclones. *Nature* **2008**, *455*, 92–95. [[CrossRef](#)] [[PubMed](#)]
- Lin, N.; Emanuel, K.; Oppenheimer, M.; Vanmarcke, E. Physically based assessment of hurricane surge threat under climate change. *Nat. Clim. Chang.* **2012**, *2*, 462–467. [[CrossRef](#)]
- Bilskie, M.V.; Hagen, S.C.; Medeiros, S.C.; Passeri, D.L. Dynamics of sea level rise and coastal flooding on a changing landscape. *Geophys. Res. Lett.* **2014**, 927–934. [[CrossRef](#)]
- Passeri, D.L.; Hagen, S.C.; Medeiros, S.C.; Bilskie, M.V. Impacts of historic morphology and sea level rise on tidal hydrodynamics in a microtidal estuary (Grand Bay, Mississippi). *Cont. Shelf Res.* **2015**, *111*, 150–158. [[CrossRef](#)]
- ARCADIS. *ADCIRC Based Storm Surge Analysis of Sea Level Rise in the Galveston Bay and Jefferson County Area in Texas*; Prepared for The Nature Conservancy; Highlands Ranch, Colorado 80129. 2011. Available online: <http://cbbep.org/publications/publication1306.pdf> (accessed on 22 November 2017).
- Cheon, S.H.; Suh, K.D. Effect of sea level rise on nearshore significant waves and coastal structures. *Ocean Eng.* **2016**, *114*, 280–289. [[CrossRef](#)]
- Heather, S. Eshorance: An Online Methodology for Estimating the Response of Estuarine Shores From Sea Level Rise. In Proceedings of the NSW Coastal Conference, Batemans Bay, NSW, Australia, 10–12 November 2010; pp. 1–16.
- Zhang, K.; Douglas, B.; Leatherman, S.; The, S.; July, N.; Zhang, K.; Douglas, B.; Leatherman, S. Do Storms Cause Long-Term Beach Erosion along the U.S. East Barrier Coast? *J. Geol.* **2002**, *110*, 493–502. [[CrossRef](#)]
- The Nature Conservancy; NOAA National Ocean Service Center. *Marshes on the Move: A Manager's Guide to Understanding and Using Model Results Depicting Potential Impacts of Sea Level Rise on Coastal Wetlands*; Washington, DC, USA, 2011. Available online: <https://coast.noaa.gov/data/digitalcoast/pdf/marshes-on-the-move.pdf> (accessed on 22 November 2017).
- Morris, J.T.; Sundareshwar, P.V.; Nietch, C.T.; Kjerfve, B.; Cahoon, D.R. Responses of coastal wetlands to rising sea level. *Ecology* **2002**, *83*, 2869–2877. [[CrossRef](#)]

21. Bertness, M.D.; Ellison, A.M. Determinants of Pattern in a New England Salt Marsh Plant Community. *Ecol. Monogr.* **1987**, *57*, 129–147. [[CrossRef](#)]
22. Cahoon, D.R.; Hensel, P.F.; Spencer, T.; Reed, D.J.; McKee, K.L.; Saintilan, N. Coastal Wetland Vulnerability to Relative Sea-Level Rise: Wetland Elevation Trends and Process Controls. *Wetl. Nat. Resour. Manag.* **2006**, *190*, 271–292. [[CrossRef](#)]
23. Kirwan, M.L.; Temmerman, S.; Skeeahan, E.E.; Guntenspergen, G.R.; Fagherazzi, S. Overestimation of marsh vulnerability to sea level rise. *Nat. Clim. Chang.* **2016**, *6*, 253–260. [[CrossRef](#)]
24. Doyle, T.W.; Krauss, K.W.; Conner, W.H.; From, A.S. Predicting the retreat and migration of tidal forests along the northern Gulf of Mexico under sea-level rise. *For. Ecol. Manag.* **2010**, *259*, 770–777. [[CrossRef](#)]
25. Williams, K.; Ewel, K.C.; Stumpf, R.P.; Putz, F.E.; Thomas, W.; Workman, T.W. Sea-level rise and coastal forest retreat on the west coast of Florida, USA. *Ecology* **2007**, *80*, 2045–2063. [[CrossRef](#)]
26. Anderson, K.E.; Cahoon, D.R.; Gill, S.K.; Gutierrez, B.T.; Thieler, E.R.; Titus, J.G.; Williams, S.J. Executive summary. In *Coastal Sensitivity to Sea-Level Rise: A Focus on the Mid-Atlantic Region*; A Report by the U.S. Climate Change Science Program and the Subcommittee on Global Change Research; U.S. Climate Change Science Program and the Subcommittee on Global Change Research: Washington, DC, USA, 2009; pp. 1–8.
27. Frey, A.E.; Olivera, F.; Irish, J.L.; Dunkin, L.M.; Kaihatu, J.M.; Ferreira, C.M.; Edge, B.L. Potential impact of climate change on hurricane flooding inundation, population affected and property damages in Corpus Christi. *J. Am. Water Resour. Assoc.* **2010**, *46*, 1049–1059. [[CrossRef](#)]
28. Woodruff, J.D.; Irish, J.L.; Camargo, S.J. Coastal flooding by tropical cyclones and sea-level rise. *Nature* **2013**, *504*, 44–52. [[CrossRef](#)] [[PubMed](#)]
29. Irish, J.L.; Frey, A.E.; Rosati, J.D.; Olivera, F.; Dunkin, L.M.; Kaihatu, J.M.; Ferreira, C.M.; Edge, B.L. Potential implications of global warming and barrier island degradation on future hurricane inundation, property damages, and population impacted. *Ocean Coast. Manag.* **2010**, *53*, 645–657. [[CrossRef](#)]
30. Mousavi, M.E.; Irish, J.L.; Frey, A.E.; Olivera, F.; Edge, B.L. Global warming and hurricanes: The potential impact of hurricane intensification and sea level rise on coastal flooding. *Clim. Chang.* **2011**, *104*, 575–597. [[CrossRef](#)]
31. Bilskie, M.V.; Hagen, S.C.; Alizad, K.; Medeiros, S.C.; Passeri, D.L.; Needham, H.F.; Cox, A. Dynamic simulation and numerical analysis of hurricane storm surge under sea level rise with geomorphologic changes along the northern Gulf of Mexico. *Earth's Futur.* **2016**. [[CrossRef](#)]
32. Epanchin-Niell, R.; Kousky, C.; Thompson, A.; Walls, M. Threatened protection: Sea level rise and coastal protected lands of the eastern United States. *Ocean Coast. Manag.* **2017**, *137*, 118–130. [[CrossRef](#)]
33. Murdukhayeva, A.; August, P.; Bradley, M.; LaBash, C.; Shaw, N. Assessment of Inundation Risk from Sea Level Rise and Storm Surge in Northeastern Coastal National Parks. *J. Coast. Res.* **2013**, *291*, 1–16. [[CrossRef](#)]
34. Barbier, E.B.; Hacker, S.D.; Kennedy, C.; Koch, E.; Stier, A.C.; Silliman, B.R. The value of estuarine and coastal ecosystem services. *Ecol. Monogr.* **2011**, *81*, 169–193. [[CrossRef](#)]
35. Zedler, J.B.; Kercher, S. Wetland Resources: Status, Trends, Ecosystem Services, and Restorability. *Annu. Rev. Environ. Resour.* **2005**, *30*, 39–74. [[CrossRef](#)]
36. Burkett, V.; Kusler, J. Climate change: Potential impacts and interactions in wetlands of United States. *J. Am. Water Resour. Assoc.* **2000**, *36*, 313–320. [[CrossRef](#)]
37. Baldwin, A.H.; Egnotovitch, M.S.; Clarke, E. Hydrologic change and vegetation of tidal freshwater marshes: Field, greenhouse, and seed-bank experiments. *Wetlands* **2001**, *21*, 519–531. [[CrossRef](#)]
38. Westerink, J.J.; Blain, C.A.; Luettich, R.A., Jr.; Scheffner, N.W. ADCIRC: An Advanced Three-Dimensional Circulation Model for Shelves Coasts and Estuaries, Report 2: Users Manual for ADCIRC-2DDI, Dredging Research Program Technical Report DRP-92-6; U.S. Army Engineers Waterways Experiment Station: Vicksburg, MS, USA, 1994.
39. Luettich, R.A., Jr.; Westerink, J.J. Implementation and Testing of Elemental Flooding and Drying in the ADCIRC Hydrodynamic Model, Final Report, 8/95, Contract # DACW39-94-M-5869; U.S. Army Corps of Engineers: Vicksburg, MS, USA, 1995.
40. Dietrich, J.C.; Bunya, S.; Westerink, J.J.; Ebersole, B.A.; Smith, J.M.; Atkinson, J.H.; Jensen, R.; Resio, D.T.; Luettich, R.A.; Dawson, C.; et al. A High-Resolution Coupled Riverine Flow, Tide, Wind, Wind Wave, and Storm Surge Model for Southern Louisiana and Mississippi. Part II: Synoptic Description and Analysis of Hurricanes Katrina and Rita. *Mon. Weather Rev.* **2010**, *138*, 378–404. [[CrossRef](#)]

41. Parris, A.; Bromirski, P.; Burkett, V.; Cayan, D.R.; Culver, M.; Hall, J.; Horton, R.; Knuuti, K.; Moss, R.; Obeysekera, J. *Global Sea Level Rise Scenarios for the United States National Climate Assessment*; Climate Program Office: Springfield, MD, USA, 2012.
42. Mitchell, M.; Hershner, C.; Julie, H.; Schatt, D.; Mason, P.; Eggington, E. *Recurrent Flooding Study for Tidewater Virginia*; Virginia Institute of Marine Science (VIMS) Center for Coastal Resources Management: Gloucester Point, VA, USA, 2013.
43. Sallenger, A.H.; Doran, K.S.; Howd, P.A. Hotspot of accelerated sea-level rise on the Atlantic coast of North America. *Nat. Clim. Chang.* **2012**, *2*, 884–888. [[CrossRef](#)]
44. Beckett, L.H.; Baldwin, A.H.; Kearney, M.S. Tidal marshes across a Chesapeake Bay subestuary are not keeping up with sea-level rise. *PLoS ONE* **2016**, *11*, e0159753. [[CrossRef](#)] [[PubMed](#)]
45. Watch, W. *Adapting to Climate Change in the Chesapeake Bay: Virginia's Experience*; STAC Workshop: Norfolk, VA, USA, 2011.
46. Paquier, A.E.; Haddad, J.; Lawler, S.; Ferreira, C.M. Quantification of the Attenuation of Storm Surge Components by a Coastal Wetland of the US Mid Atlantic. *Estuaries Coasts* **2017**, *40*, 930–946. [[CrossRef](#)]
47. NOAA. *Detailed Method for Mapping Sea Level Rise Marsh Migration*; NOAA: Silver Spring, MD, USA, 2017.
48. Marcy, D.; Brooks, W.; Draganov, K.; Hadley, B.; Herold, N.; McCombs, J.; Pendleton, M.; Ryan, S.; Sutherland, M.; Waters, K. *New Mapping Tool and Techniques for Visualizing Sea Level Rise and Coastal Flooding Impacts. Copyright ASCE 2011 Solutions to Coastal Disasters*; American Society of Civil Engineers (ASCE): Charleston, SC, USA, 2011; pp. 474–490.
49. Kirwan, M.L.; Murray, A.B. A coupled geomorphic and ecological model of tidal marsh evolution. *Proc. Natl. Acad. Sci. USA* **2007**, *104*, 6118–6122. [[CrossRef](#)] [[PubMed](#)]
50. D'Alpaos, A.; Lanzoni, S.; Marani, M.; Rinaldo, A. Landscape evolution in tidal embayments: Modeling the interplay of erosion, sedimentation, and vegetation dynamics. *J. Geophys. Res. Earth Surf.* **2007**, *112*, 1–17. [[CrossRef](#)]
51. Schile, L.M.; Callaway, J.C.; Morris, J.T.; Stralberg, D.; Thomas Parker, V.; Kelly, M. Modeling tidal marsh distribution with sea-level rise: Evaluating the role of vegetation, sediment, and upland habitat in marsh resiliency. *PLoS ONE* **2014**, *9*, e0088760. [[CrossRef](#)] [[PubMed](#)]
52. Craft, C.; Clough, J.; Ehman, J.; Jove, S.; Park, R.; Pennings, S.; Guo, H.; Machmuller, M. Forecasting the effects of accelerated sea-level rise on tidal marsh ecosystem services. *Front. Ecol. Environ.* **2009**, *7*, 73–78. [[CrossRef](#)]
53. NOAA-CSC C-CAP Land Cover Atlas. Available online: <https://coast.noaa.gov/digitalcoast/tools/lca.html> (accessed on 24 May 2017).
54. Booij, N.; Ris, R.C.; Holthuijsen, L.H. A third-generation wave model for coastal regions: 1. Model description and validation. *J. Geophys. Res.* **1999**, *104*, 7649–7666. [[CrossRef](#)]
55. Dietrich, J.C.; Zijlema, M.; Westerink, J.J.; Holthuijsen, L.H.; Dawson, C.; Luettich, R.A.; Jensen, R.E.; Smith, J.M.; Stelling, G.S.; Stone, G.W. Modeling hurricane waves and storm surge using integrally-coupled, scalable computations. *Coast. Eng.* **2011**, *58*, 45–65. [[CrossRef](#)]
56. Dietrich, J.C.; Tanaka, S.; Westerink, J.J.; Dawson, C.N.; Luettich, R.A.; Zijlema, M.; Holthuijsen, L.H.; Smith, J.M.; Westerink, L.G.; Westerink, H.J. Performance of the unstructured-mesh, SWAN+ ADCIRC model in computing hurricane waves and surge. *J. Sci. Comput.* **2012**, *52*, 468–497. [[CrossRef](#)]
57. Hanson, J.L.; Wadman, H.M.; Blanton, B.; Roberts, H. *Coastal Storm Surge Analysis: Modeling System Validation*; Report 4: Intermediate Submission No. 2.0. US Army Engineer Research and Development Center (ERDC). 2013. Available online: <http://www.dtic.mil/dtic/tr/fulltext/u2/a583150.pdf> (accessed on 22 November 2017).
58. Blanton, B.; Stillwell, L.; Roberts, H.; Atkinson, J.; Zou, S.; Forte, M.; Hanson, J.; Luettich, R. *Coastal Storm Surge Analysis: Computational System Coastal and Hydraulics Laboratory*; Report 2: Intermediate Submission No. 1.2. US Army Engineer Research and Development Center (ERDC). 2011. Available online: <http://acwc.sdp.sirsi.net/client/search/asset/1000839;jsessionid=6B9DCD6BB30B93C5752FEB1B865E6A2E.enterprise-15000> (accessed on 22 November 2017).
59. Forte, M.; Hanson, J.; Stillwell, L.; Blanchard-Montgomery, M.; Blanton, B.; Luettich, R.; Roberts, H.; Atkinson, J.; Miller, J. *Coastal Storm Surge Analysis System: Digital Elevation Model*; Report 1: IDS No. 1.1; US Army Engineer Research and Development Center (ERDC). 2011. Available online: <http://acwc.sdp.sirsi.net/client/search/asset/1000838;jsessionid=6B9DCD6BB30B93C5752FEB1B865E6A2E.enterprise-15000> (accessed on 22 November 2017).

60. Le Provost, C.; Genco, M.L.; Lyard, F.; Vincent, P.; Canceil, P. Spectroscopy of the world ocean tides from a finite element hydro dynamic model. *J. Geophys. Res.* **1994**, *99*, 24777–24797. [[CrossRef](#)]
61. Nadal-caraballo, N.C.; Melby, J.A.; Gonzalez, V.M.; Cox, A.T. *Coastal Storm Hazards from Virginia to Maine Coastal and Hydraulics Laboratory*; US Army Engineer Research and Development Center (ERDC). 2015. Available online: http://www.nad.usace.army.mil/Portals/40/docs/ComprehensiveStudy/Coastal_Storm_Hazards_from_Virginia_to_Maine.pdf (accessed on 22 November 2017).
62. Mattocks, C.; Forbes, C.; Ran, L. *Design and Implementation of a Real-Time Storm Surge and Flood Forecasting Capability for the State of North Carolina*; 2006. Available online: http://www.unc.edu/ims/adcirc/publications/2006/2006_Mattocks.pdf (accessed on 22 November 2017).
63. Mattocks, C.; Forbes, C. A real-time, event-triggered storm surge forecasting system for the state of North Carolina. *Ocean Model.* **2008**, *25*, 95–119. [[CrossRef](#)]
64. Holland, G.J. An analytical model of the wind and pressure profiles in hurricanes. *Mon. Weather Rev.* **1980**, *108*, 1212–1218. [[CrossRef](#)]
65. NOAA NOAA Tides & Currents. Available online: <https://tidesandcurrents.noaa.gov/> (accessed on 26 April 2018).
66. Garzon, J.; Ferreira, C. Storm Surge Modeling in Large Estuaries: Sensitivity Analyses to Parameters and Physical Processes in the Chesapeake Bay. *J. Mar. Sci. Eng.* **2016**, *4*, 45. [[CrossRef](#)]
67. Xiong, Y.; Berger, C.R. Chesapeake Bay Tidal Characteristics. *J. Water Resour. Prot.* **2010**, *02*, 619–628. [[CrossRef](#)]
68. Atkinson, J.; McKee Smith, J.; Bender, C. Sea-Level Rise Effects on Storm Surge and Nearshore Waves on the Texas Coast: Influence of Landscape and Storm Characteristics. *J. Waterw. Port Coast. Ocean Eng.* **2013**, *139*, 98–117. [[CrossRef](#)]
69. Passeri, D.L.; Hagen, S.C.; Plant, N.G.; Bilskie, M.V.; Medeiros, S.C.; Alizad, K. Tidal hydrodynamics under future sea level rise and coastal morphology in the Northern Gulf of Mexico. *Earth's Futur.* **2016**, *4*, 159–176. [[CrossRef](#)]
70. Atkinson, J.; Ph, D.; Hagen, S.C.; Ce, D.; Wre, D.; Zou, S.; Bacopoulos, P.; Medeiros, S.; Weishampel, J. Deriving Frictional Parameters and Performing Historical Validation for an ADCIRC Storm Surge Model of the Florida Gulf Coast. *Florida Watershed* **2011**, *4*, 22–27.
71. Ferreira, C.M. Uncertainty in hurricane surge simulation due to land cover specification. *J. Geophys. Res. Ocean.* **2014**, *119*, 1812–1827. [[CrossRef](#)]
72. Ferreira, C.M.; Olivera, F.; Irish, J.L. Arc StormSurge: Integrating Hurricane Storm Surge Modeling and GIS. *J. Am. Water Resour. Assoc.* **2014**, *50*, 219–233. [[CrossRef](#)]
73. Xia, M.; Xie, L.; Pietrafesa, L.J.; Peng, M. A Numerical Study of Storm Surge in the Cape Fear River Estuary and Adjacent Coast. *J. Coast. Res.* **2008**, *4*, 159–167. [[CrossRef](#)]
74. Li, H.; Lin, L.; Burks-Copes, K. Numerical modeling of coastal inundation and sedimentation by storm surge, tides, and waves at Norfolk, Virginia, USA. In Proceedings of the 33rd International Conference on Coastal Engineering, Santander, Spain, 1–6 July 2012.
75. Zhang, K.; Li, Y.; Liu, H.; Xu, H.; Shen, J. Comparison of three methods for estimating the sea level rise effect on storm surge flooding. *Clim. Chang.* **2013**, *118*, 487–500. [[CrossRef](#)]
76. Glass, E.M.; Garzon, J.L.; Lawler, S.; Paquier, E.; Ferreira, C.M. Potential of marshes to attenuate storm surge water level in the Chesapeake Bay. *Limnol. Oceanogr.* **2017**. [[CrossRef](#)]
77. Kennedy, V.S.; Twilley, R.R.; Kleypas, J.A.; Cowan, J.H.; Hare, S.R. *Coastal and Marine Ecosystems and Global Climate Change: Potential Effects on U.S. Resources*; Prepared for the Pew Center on Global Climate Change; Center for Climate and Energy Solutions: Arlington, VA, USA, 2002; p. 64.
78. Glick, P.; Clough, J.; Polaczyk, A.; Couvillion, B.; Nunley, B. Potential Effects of Sea-Level Rise on Coastal Wetlands in Southeastern Louisiana. *J. Coast. Res. Spec. Issue 63 Underst. Predict. Chang. Coast. Ecosyst. North. Gulf Mex.* **2013**, *63*, 211–233. [[CrossRef](#)]

